Influence of confined phonon modes on the thermal behavior of AlAs/GaAs quantum cascade structures

C. Becker, C. Sirtori,* H. Page, A. Robertson, V. Ortiz, and X. Marcadet
Thales Research & Technology, Domaine de Corbeville, 91404 Orsay, France
(Received 20 August 2001; published 30 January 2002)

The thermal behavior of AlAs/GaAs quantum cascade structures is used to demonstrate the existence of confined and interface optical-phonon modes. The high conduction-band offset of this material system greatly improves the confinement of the electronic states and allows the realization of electroluminescence structures, where the optical power as a function of the temperature solely depends on the change of the upper-state lifetime induced by the longitudinal-optical-phonon population. We observed that the latter is proportional to the Bose-Einstein factor, with an appropriate phonon mode energy, which does not simply correspond to that of the GaAs bulk phonon (36-meV energy). In particular we show that the agreement between theory and experiment can be substantially improved when the confined and interface modes are taken into account in our calculation. Our results are corroborated by the threshold temperature dependence of lasers, with an active region based on similar structures.

DOI: 10.1103/PhysRevB.65.085305 PACS number(s): 63.20.Kr, 63.20.Pw, 42.72.Ai

During recent years, many aspects of the physics controlling population inversion between subbands in quantum cascade (QC) structures have been intensively studied and clarified.[1–6] However, until now, to our best knowledge, there is no evident explanation of its thermal behavior, which is not simply relative to the variation with temperature of the subband lifetimes. Different dependencies have been measured for different active region designs and material systems. To explain the discrepancy between experimental results and theoretical predictions, temperature-activated phenomena have been invoked, which hinder population inversion[7] or induce nonunity injection efficiency of electrons in the excited state of the laser transition.[6] In order to minimize the spurious effect coming from parallel current paths and have a better measure of the phonon effects on the subband lifetime, we have designed a QC active region based on a high conduction-band-offset material system AlAs/GaAs,[8] so to increase the activation barrier ''seen'' by the electrons and avoid current leakage. These devices show a thermal behavior, which is solely controlled by the optical-phonon-limited lifetime of the upper state of the laser transition. In this paper, we show that the differential efficiency (dP/dI) of the spontaneous emission follows the Bose-Einstein dependence of the phonon population with the temperature, up to 300 K, the maximum temperature of our experiment. This thermal dependence is also reflected in laser structures where the threshold current shows the same phonon-limited behavior.[8] However, the phonon energy that best fits our data is slightly higher than the expected 36 meV (the longitudinal-optical-phonon energy in bulk GaAs). We address this problem by developing self-consistent calculations of the phonon modes within the framework of the dielectric continuum model,[9] which gives a better agreement with the experimental results and confirms the presence of interface and confined phonon modes.

The active region of our AlAs/GaAs structure consists of three wells coupled by tunneling to a manifold of states through a 1.9-nm-thick injection barrier as described in detail in Ref. 8. In Fig. 1, we show a schematic band diagram of the active region of our structure as well as the moduli squared of the most relevant wave functions. In this material system, the Γ-point conduction-band offset is ~1 eV, which enables us to better confine the energy states of the active region and to suppress thermally activated parallel current paths.[8] The $n=4$ state is more than 70 meV higher in energy than the excited state of the laser transition (see Fig. 1). However, this state is very well confined within the three wells that define the active region and is very unlikely to contribute to the transport. More importantly, the bottom of the manifold of states above the active region, which we believe is the main channel for the thermally activated escape of electrons, is situated 120 meV above the state $n=3$ (ΔE_{act} in Fig. 1). An indirect proof of the absence of thermally activated leakage currents has been already evidenced by the fact that the slope efficiency of lasers based on this heterostructure is nearly constant with the temperature.[8] In such devices, therefore, it should be possible to describe the thermal behavior only in terms of electron-optical-phonon scattering.

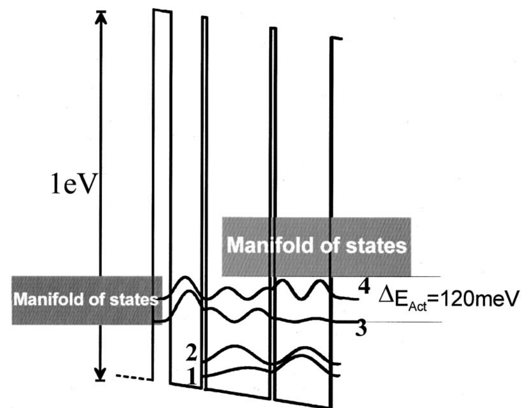

FIG. 1. Conduction-band energy diagram of the active region of the quantum cascade structure under an applied electric field $F = 39\,\mathrm{kV/cm}$. Shown are the moduli squared of the relevant wave functions. The layer sequence, in nanometers, from left to right starting from the first GaAs well, is 33/**5**/68/**5**/60. AlAs layers are in bold.

 ©2002 The American Physical Society

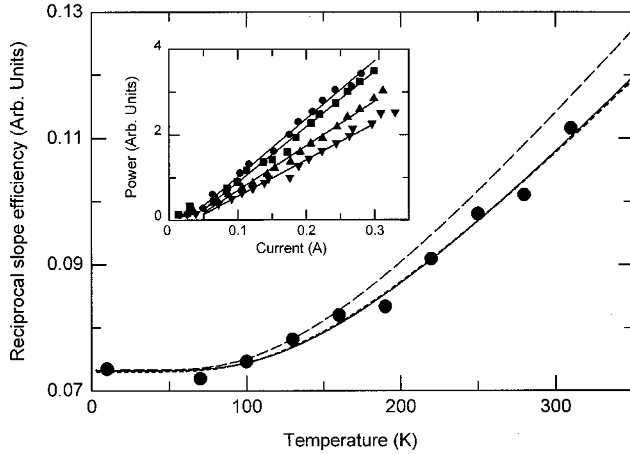

FIG. 2. Reciprocal slope efficiency of the electroluminescence measured as a function of the temperature. The solid line is the result of a fit of the experimental data by Eq. (3) and the obtained value for the phonon energy is 39 meV. The dashed line corresponds to Eq. (3) of the text, with $\hbar\omega$ imposed equal to 36 meV. The dotted line corresponds to Eq. (6) of the text, with equivalent modes calculated at 36 and 47 meV for this structure. In the inset is shown the luminescence signal as a function of the current, obtained as described in the text. The circles, squares, and up and down triangles correspond, respectively, to measurements at 10, 100, 220, and 310 K. The solid lines represent the linear fit of the data over the range of current 50–300 mA.

In order to characterize the thermal behavior of our structure, we have measured the integrated light emitted by an electroluminescent device, which consisted of 10 periods of the injector/active region sequence, surrounded by two highly doped GaAs contact layers and grown on a semi-insulating GaAs substrate. The samples were processed into circular mesas of 120-μm diameter, provided with Au/Ge/Ni contact. One edge of the sample was ground at an angle of 45° to extract the light from the substrate. Above 200 K, a polarizer was used to separate the parasitic black-body radiation arising from bulk heating effects in the structure from the intersubband signal. The intersubband signal is polarized perpendicular to the plane of the layers and therefore, by subtracting the curves measured with crossed polarizations, we can extract our signal without spurious contributions. In the absence of optical feedback the intersubband light intensity scales linearly over a wide range of current. This can be seen in the inset of Fig. 2, where we have plotted the luminescence signal as a function of the injected current for different temperatures (10, 100, 220, and 310 K). At low currents (<50 mA), however, the signal shows a superlinear behavior. This is explained by the fact that, at low applied bias, a fraction of the electrons is injected directly into state $n=2$ (see Fig. 1) and the ratio between this parasitic injection and the direct injection into state $n=3$ changes as the field across the structure increases. Once the bias has aligned the injector and level $n=3$, electrons tunnel resonantly into the latter and the leak into the $n=2$ state becomes negligible.

The measurement of the luminescence signal in mesa-type structures, where no optical feedback occurs, is equivalent to a measure of the spontaneous emission. The latter is proportional to the population into the $n=3$ state and the differential efficiency is directly related to the nonradiative lifetime of electrons on this state by the relation[10]

$$\frac{dP}{dI}(T)=\frac{\hbar\omega}{e}\frac{\tau_3(T)}{\tau_{\rm rad}}N_p\eta, \tag{1}$$

where $\hbar\omega$ is the energy of the emitted photons, $\tau_{\rm rad}$ is the spontaneous emission lifetime, which is insensitive to temperature, N_p is the number of periods, and η is the collection efficiency of the optical system. In Eq. (1), we have assumed that the energy position of the peak is nearly constant with the temperature. Although this is not exactly true, this approximation holds because the change of energy between 4 and 300 K is less than 3%. In our case, τ_3 is controlled by the optical-phonon-electron scattering. If the distance in energy between the subbands is bigger than the optical-phonon energy, both the emission and the absorption of a phonon are possible. In this case, the thermal dependence of τ_3 reads

$$\tau_3{}^{-1}(T)=\tau_{3,e}{}^{-1}(0)(1+n(T))+\tau_{3,a}{}^{-1}(0)\cdot n(T), \tag{2}$$

where $\tau_{3,e}(0)$ $[\tau_{3,a}(0)]$ is the scattering time for the emission (absorption) of a phonon at $T=0$ K and $n(T)$ is the phonon population at the temperature T. The phonon population is given by a Bose-Einstein factor and the temperature dependence of τ_3 in the case of a single phonon mode with energy $\hbar\omega_{\rm LO}$ is then given by

$$\tau_3{}^{-1}(T)=\tau_{3,e}{}^{-1}(0)\left[1+\frac{1}{\exp\left(\frac{\hbar\omega_{\rm LO}}{kT}\right)-1}\right]+\tau_{3,a}{}^{-1}(0)\cdot\frac{1}{\exp\left(\frac{\hbar\omega_{\rm LO}}{kT}\right)-1}, \tag{3}$$

where k is the Boltzmann constant. In our calculation of $\tau_3{}^{-1}(0)$, we have included the contributions of the scattering processes with all relevant states in the active region and in the downstream injector.

Following Eq. (1), we have done a linear fit of the power as a function of the current to extract the slope efficiency over the range of current 50–300 mA as stressed by the solid lines in the inset of Fig. 2. In this figure, we also report the inverse of the slope efficiency as a function of the temperature. The solid line in Fig. 2 is the best fit of the experimental results with Eq. (3), using $\hbar\omega_{\rm LO}$ as the free parameter. The result of the fit gives an energy $\hbar\omega_{\rm LO}$ equal to 39 meV. This value does not correspond to the energy of longitudinal-optical phonons in bulk GaAs ($\hbar\omega_{\rm LO}=36$ meV). The dashed line on the same graph corresponds to Eq. (3) with $\hbar\omega=36$ meV. We explain the discrepancy between this last curve and the experimental data by the fact that the bulk treatment for the phonons in the AlAs/GaAs material system is not accurate, as already proven by Raman measurements.[11–13]

In heterostructures where a strong difference between the dielectric constants of the materials is present, more precise values of the phonon-scattering rates can be derived within

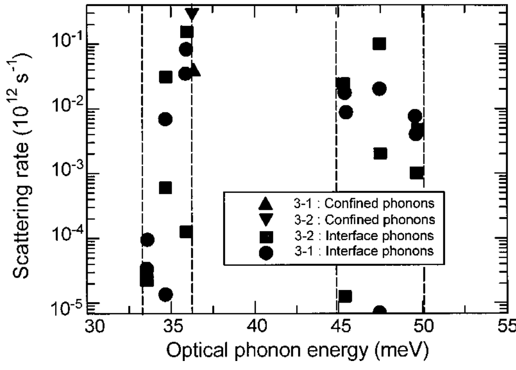

FIG. 3. Electron-optical-phonon scattering rates for the confined and interface phonon modes and for both 3-2 and 3-1 transitions, calculated within the framework of the dielectric continuum model. The squares and the circles correspond to the interface phonons for transitions 3-2 and 3-1, respectively. The down and up triangles correspond to the confined phonons for transitions 3-2 and 3-1, respectively.

the framework of the macroscopic dielectric continuum model.[9] In this model, phonons are described as confined and interface modes. The confined modes for each well are calculated by the method of Huang and Zhu.[9] For the interface phonon modes, however, a self-consistent calculation similar to the transfer-matrix method from Yu *et al.*[14] was developed. In the case of emission or absorption of a longitudinal-optical (LO) phonon by an intersubband electronic transition, the wave vector of the interface phonon depends on the distance in energy between the subbands ΔE and the phonon energy $\hbar\omega_{\mathrm{LO}}$ through the relation

$$k_{\parallel}=\frac{\sqrt{2m^{*}(\Delta E\pm\hbar\omega_{\mathrm{LO}})}}{\hbar},\tag{4}$$

where m^{*} is the effective mass of the electrons. The sign $+$ $(-)$ corresponds to the case of the emission (absorption). However, the values of $\hbar\omega_{\mathrm{LO}}$ are not known beforehand during the calculation of the interface phonon modes. Therefore, it is necessary to treat the problem in a self-consistent way. In our method, we start by solving the Schrödinger equation in the effective-mass approximation, and then self-consistently solve the equations for the interface phonon mode frequencies and their wave vectors. The scattering rates associated with the emission of a phonon in each mode for the 3-2 and 3-1 transitions are shown in Fig. 3. The dashed lines are placed at the energy of $\hbar\omega_{\mathrm{TO,GaAs}}\approx 33$, $\hbar\omega_{\mathrm{LO,GaAs}}\approx 36$, $\hbar\omega_{\mathrm{TO,AlAs}}\approx 45$, and $\hbar\omega_{\mathrm{LO,AlAs}}\approx 50$ meV.[14] For the 3-1 transition, the confined modes contribution is small compared to that of the interface modes (~five times lower). This is due to the presence of a thin AlAs barrier between the two wide wells in the active region, playing the role of a phonon wall.[15] The total scattering rate is then reduced from 3.6×10^{11} s^{-1} in the bulk phonon model to 2.2×10^{11} s^{-1}. For the 3-2 transition however, the scattering time calculated in the dielectric continuum model (1.6 ps) is shorter than that obtained with bulk calculations (1.9 ps). The total scattering time τ_3 for the state $n=3$ is at the end almost the same in the two models (1.1 ps for the bulk model and 1.2 ps for the other). In the framework of our calculations, τ_3 as a function of the temperature is given by the relation

$$\tau_3^{-1}(T)=\sum_i \tau_{3,e,E_i}{}^{-1}(0)\cdot\left[1+\frac{1}{e^{E_i/kT}-1}\right]+\sum_i \tau_{3,a,E_i}{}^{-1}(0)\cdot\frac{1}{e^{E_i/kT}-1},\tag{5}$$

where $\tau_{3,e,E_i}{}^{-1}(0)$ $[\tau_{3,a,E_i}{}^{-1}(0)]$ is the scattering rate at $T=0$ K of the electrons by the emission (absorption) of a phonon in the mode of energy E_i. As can be seen in Fig. 3, in the specific case of our structure, two phonon modes, at 36 and 47 meV, dominate the scattering rate. Thus, we can reduce the right part of Eq. (5) to a sum of four terms and describe the thermal dependence of τ_3 by introducing those effective modes. These two modes correspond to the sum of all the GaAs- and AlAs-like modes, respectively. In this case, the dependence reads

$$\tau_3^{-1}(T)=\tau_{3,e}{}^{-1}(T)+\tau_{3,a}{}^{-1}(T),$$

$$\tau_{3,e}{}^{-1}(T)=\tau_{3,e,36\ \mathrm{meV}}{}^{-1}(0)\left[1+\frac{1}{\exp\left(\frac{36\ \mathrm{meV}}{kT}\right)-1}\right]+\tau_{3,e,47\ \mathrm{meV}}{}^{-1}(0)\left[1+\frac{1}{\exp\left(\frac{47\ \mathrm{meV}}{kT}\right)-1}\right],$$

$$\tau_{3,a}{}^{-1}(T)=\tau_{3,a,36\ \mathrm{meV}}{}^{-1}(0)\cdot\frac{1}{\exp\left(\frac{36\ \mathrm{meV}}{kT}\right)-1}+\tau_{3,a,47\ \mathrm{meV}}{}^{-1}(0)\cdot\frac{1}{\exp\left(\frac{47\ \mathrm{meV}}{kT}\right)-1},\tag{6}$$

where $\tau_{3,e,36\,\mathrm{meV}}{}^{-1}(0)$ $[\tau_{3,a,36\,\mathrm{meV}}{}^{-1}(0)]$ is the sum of the confined phonons and the GaAs-like interface modes scattering rates for the emission (absorption) of a phonon at $T=0$ K and $\tau_{3,e,47\,\mathrm{meV}}{}^{-1}(0)$ $[\tau_{3,a,47\,\mathrm{meV}}{}^{-1}(0)]$ is the total rate for the emission (absorption) of AlAs-like interface phonons at zero temperature.

The dotted line in Fig. 2 corresponds to Eq. (6) for the phonon modes and scattering rates calculated for this structure. The agreement with the experimental data is noticeably better over the whole range of temperature. This confirms that the phonon population in the structure is correctly described by taking into account both confined and interface phonons, even though the effect on the lifetime of the $n=3$ state at 0 K is negligible.

The same formalism can be also used to describe the thermal behavior of lasers with similar active regions.[8] In these lasers, the threshold current density scales linearly between 130 and 230 K and is practically constant between 0 and

100 K. Electron-phonon scattering induces a thermal dependence of the threshold current density by means of τ_3 as shown by the simplified relation

$$J_{th}=\frac{e}{\tau_3}\cdot\frac{\alpha}{g_c}, \tag{7}$$

obtained by rate equations.[16] Here, e is the electron charge, α (in cm^{-1}) represents the total optical losses and is the sum of the waveguide and the mirror losses, and g_c (in cm) is the gain cross section as defined in Ref. 16. In Eq. (7), we have assumed that τ_{32} is much bigger than τ_2 and that no thermal-activated processes are present as discussed before.

The waveguide losses in QC lasers are independent from the temperature and therefore the temperature-dependent parameters in Eq. (7) are only the electronic lifetime τ_3 and the gain cross section. We assume here that the latter is inversely proportional to the broadening $2\gamma_{32}$ of the transition, given by the measured full width at half maximum (FWHM) of the luminescence peak, which is determined by measuring the spontaneous emission from a side of the ridge. The linewidth for each temperature was measured at the threshold voltage. The results are shown in the inset of Fig. 4 where the luminescence FWHM is plotted against the temperature, going from 13.4 meV at 10 K to 17.5 meV at 230 K.

It is possible to obtain a parameter directly related to the electron-optical-phonon interaction by combining the thermal dependence of the gain cross section with that of the threshold current density. In Fig. 4, we show the threshold current density divided by the luminescence FWHM ($2\gamma_{32}$) plotted against the temperature. On this graph is also plotted the curve corresponding to Eq. 6 (solid line). The agreement between the calculations and the experimental data is very good. Note however that the experimental curve decreases for $T>200$ K, a behavior that is not predicted by the theory. We believe that this is due to an overestimate of the gain width at $T>200$ K, because the FWHM of the luminescence peak increases too rapidly. This may be related to the fact that the threshold voltage increases with the temperature, leading to an over-increase of the linewidth of the measured transition.

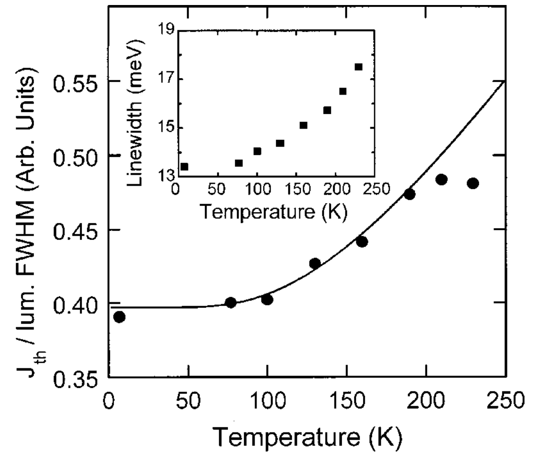

FIG. 4. Threshold current density divided by the luminescence FWHM as a function of temperature. The solid line corresponds to Eq. (6) of the text. In the inset is shown the measured luminescence FWHM for different temperatures.

In conclusion, we showed that the thermal behavior of AlAs/GaAs quantum cascade structures can be explained by the temperature-dependent electron-optical-phonon scattering. The threshold current density of a laser and the slope efficiency of the electroluminescence of a diode can be used as a signature of the confined and interface phonon populations in the structure.

We are grateful to Jerome Faist for his useful comments on the paper. This work was partly supported by the European Community by Research Project No. SUPERSMILE IST-1999-1493.

*Corresponding author: Email address: carlo.sirtori@thalesgroup.com

[1] J. Faist, F. Capasso, C. Sirtori, D. L. Sivco, J. N. Baillargeon, A. L. Hutchinson, S.-N. G. Chu, and A. Y. Cho, Appl. Phys. Lett. **68**, 3680 (1996); J. Faist, F. Capasso, C. Sirtori, D. L. Sivco, A. L. Hutchinson, M. S. Hybertsen, and A. Y. Cho, Phys. Rev. Lett. **68**, 3680 (1996).

[2] B. Gelmont, V. B. Gorfinkel, and S. Luryi, Appl. Phys. Lett. **68**, 2171 (1996).

[3] V. F. Elesin and A. V. Krasheninnikov, Zh. Eksp. Teor. Fiz. **111**, 681 (1997) [JETP Lett. **84**, 375 (1997)].

[4] G. Paulavicius, V. Mitin, and M. A. Stroscio, J. Appl. Phys. **84**, 3459 (1998).

[5] S. Slivken, V. I. Litvinov, M. Razeghi, and J. R. Meyer, J. Appl. Phys. **85**, 665 (1999).

[6] H. Page, C. Becker, A. Robertson, G. Glastre, V. Ortiz, and C. Sirtori, Appl. Phys. Lett. **78**, 3529 (2001).

[7] J. Faist, F. Capasso, C. Sirtori, D. L. Sivco, A. L. Hutchinson, and A. Y. Cho, Appl. Phys. Lett. **66**, 538 (1995).

[8] C. Becker, C. Sirtori, H. Page, G. Glastre, V. Ortiz, X. Marcadet, M. Stellmacher, and J. Nagle, Appl. Phys. Lett. **77**, 463 (2000).

[9] K. Huang and B. Zhu, Phys. Rev. B **38**, 13 377 (1988).

[10] C. Sirtori, F. Capasso, J. Faist, D. L. Sivco, A. L. Hutchinson, and A. Y. Cho, Appl. Phys. Lett. **66**, 4 (1995).

[11] A. J. Shields, M. Cardona, and K. Eberl, Phys. Rev. Lett. **72**, 412 (1994).

[12] A. J. Shields, M. P. Chamberlain, M. Cardona, and K. Eberl, Phys. Rev. B **51**, 17 728 (1995).

[13] V. F. Sapega, M. P. Chamberlain, T. Ruf, M. Cardona, D. N. Mirlin, K. Tötemeyer, A. Fischer, and K. Eberl, Phys. Rev. B **52**, 14 144 (1995).

[14] S. Yu, K. W. Kim, M. A. Stroscio, G. J. Iafrate, J.-P. Sun, and G. I. Haddad, J. Appl. Phys. **82**, 3363 (1997).

[15] B. K. Ridley, Appl. Phys. Lett. **66**, 3633 (1995).

[16] J. Faist, F. Capasso, C. Sirtori, D. L. Sivco, and A. Y. Cho, in *Intersubband transitions in Quantum Wells: Physics and Device Applications* II, Semiconductors and Semimetals Vol. 66 (Academic, New York, 2000).